

# New insight into the exotic states strongly coupled with the $D\bar{D}^*$ from the $T_{cc}^+$

Guang-Juan Wang,<sup>1,\*</sup> Zhi Yang,<sup>2,†</sup> Jia-Jun Wu,<sup>3,‡</sup> Makoto Oka,<sup>4,5,§</sup> and Shi-Lin Zhu<sup>6,¶</sup>

<sup>1</sup>KEK Theory Center, Institute of Particle and Nuclear Studies (IPNS), High Energy Accelerator Research Organization (KEK), 1-1 Oho, Tsukuba, Ibaraki, 305-0801, Japan

<sup>2</sup>School of Physics, University of Electronic Science and Technology of China, Chengdu 610054, China

<sup>3</sup>School of Physical Sciences, University of Chinese Academy of Sciences (UCAS), Beijing 100049, China

<sup>4</sup>Advanced Science Research Center, Japan Atomic Energy Agency, Tokai, Ibaraki, 319-1195, Japan

<sup>5</sup>Nishina Center for Accelerator-Based Science, RIKEN, Wako 351-0198, Japan

<sup>6</sup>School of Physics and Center of High Energy Physics, Peking University, Beijing 100871, China

(Dated: July 3, 2024)

We have investigated the internal structure of the open- and hidden-charmed ( $DD^*/\bar{D}D^*$ ) molecules in the unified framework. We first fit the experimental lineshape of the  $T_{cc}^+$  state and extract the  $DD^*$  interaction, from which the  $T_{cc}^+$  is assumed to arise solely. Then we obtain the  $D\bar{D}^*$  interaction by charge conjugation. Our results show that the  $D\bar{D}^*$  interaction is attractive but insufficient to form  $X(3872)$  as a bound state. Instead, its formation requires the crucial involvement of the coupled channel effect between the  $D\bar{D}^*$  and  $c\bar{c}$  components, although the  $c\bar{c}$  accounts for approximately 1% only. Besides  $X(3872)$ , we have obtained a higher-energy state around 3957.9 MeV with a width of 16.7 MeV, which may be a potential candidate for the  $X(3940)$ . In  $J^{PC} = 1^{+-}$  sector, we have found two states related to the iso-scalar  $\tilde{X}(3872)$  and  $h_c(2P)$ , respectively. Our combined study provides valuable insights into the nature of these  $DD^*/D\bar{D}^*$  exotic states.

## I. INTRODUCTION

The exotic states, which are beyond the simple quark model pictures of the quark-antiquark meson and three-quark baryon, have greatly enriched the hadron spectroscopy. Their inner structures remain a mystery and the investigations of their dynamics have been an ongoing and central issue in the study of nonperturbative Quantum Chromodynamics (QCD).

One of the most well-known exotic states is the  $X(3872)$  with  $J^{PC} = 1^{++}$  (also named as  $\chi_{c1}(3872)$  in RPP [1]), which was first observed by the Belle Collaboration in 2003 [2] and subsequently confirmed by various experimental collaborations [3–8]. It is located extremely near the  $D^0\bar{D}^{*0}$  <sup>1</sup> threshold, with a mass difference of  $M_{X(3872)} - M_{D^0\bar{D}^{*0}} = 0 \pm 0.18$  MeV. The location is also not too far away from the  $\chi_{c1}(2P)$  meson predicted by the Godfrey-Isgur (GI) relativized quark model [9], with  $M_{\chi_{c1}(2P)} - M_{X(3872)} = 81.4$  MeV. So far, there are different theoretical interpretations, such as the conventional twisted  $\chi_{c1}(2P)$  charmonium [10, 11], the compact tetraquark state, the  $D^*\bar{D}/D\bar{D}^*$  molecule [12–15], the mixture of the  $c\bar{c}$  and  $D^*\bar{D}/D\bar{D}^*$  molecule [16–23]. For more details, see Refs. [24–28] for reviews.

The  $X(3872)$  is challenging to understand due to its proximity to the  $D\bar{D}^*$  threshold and the intricate interactions between the components  $c\bar{c}$  and the  $D\bar{D}^*$ . In traditional methods, the parameters governing the  $D\bar{D}^*$  in-

teraction are often estimated through phenomenological models, leading to substantial uncertainties, especially for the near-threshold states. Within the molecular scenario, there are two possible fine-tuning mechanisms for the  $X(3872)$ : either the accidental fine-tuning of the parameters in the  $D\bar{D}^*$  sector or an accidental fine-tuning of a P-wave  $c\bar{c}$  meson to the  $D\bar{D}^*$  threshold [16]. Without constraints on these two parts, determining their roles solely based on limited observables is practically impossible. This work will address this question with the  $T_{cc}^+$  and  $\psi(3770)$  ( $^3D_1$ ) experimental data.

The  $T_{cc}^+$  was recently reported by LHCb collaboration in the  $D^0D^0\pi^+$  channel [29, 30] and has attracted a great deal of interest [31–54]. Since the  $T_{cc}^+$  is located just below the  $D^0D^{*+}$  threshold within several hundred keV, the  $DD^*$  interaction definitely plays the most important role in the formation of this exotic state, offering precious experimental data to constrain the  $DD^*$  interaction.

To combine the strength of experimental data with a direct connection between  $DD^*$  and  $D\bar{D}^*$ , we first perform a detailed analysis of the  $D^0D^0\pi$  invariant mass for the  $T_{cc}^+$  distributions considering the dynamical complexities of the  $DD^*$  interaction. Our approach employs a coupled-channel formalism and incorporates comprehensive scattering potentials, including the exchanges of light mesons ( $\pi$ ,  $\rho$ ,  $\omega$ ). These  $D\bar{D}^*$  potentials are derived from a heavy hadron effective Lagrangian and  $D\bar{D}^*$  interactions can be directly obtained with the charge conjugation symmetry. The potential coupling of  $c\bar{c}$  with  $D\bar{D}^*$  happens through the quark-pair creation (QPC) model, which is determined through the well-studied  $c\bar{c}$  state  $\psi(3770)$  ( $^3D_1$ ).

\* wgj@post.kek.jp

† zhiyang@uestc.edu.cn, corresponding author

‡ wujiajun@ucas.ac.cn, corresponding author

§ makoto.oka@riken.jp

¶ zhushl@pku.edu.cn

<sup>1</sup> Hereafter, we use the notion  $D\bar{D}^*$  to represent  $D\bar{D}^*+c.c..$

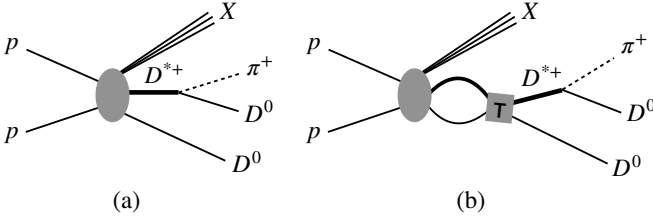


FIG. 1. The Feynman diagram for  $pp \rightarrow D^0 D^0 \pi^+ X$  ( $X$  denotes all the produced particles other than the  $D^0$ ,  $D^0$  and  $\pi^+$  in the collision). The square labeled as  $T$  denotes the scattering  $T$ -matrix for the  $D^0 D^{*+}$  and  $D^+ D^{*0}$  channels.

## II. MATERIALS AND METHODS

We first concentrate on the  $DD^*/D\bar{D}^*$  interaction. The  $S$ -wave  $DD^*$  and  $D\bar{D}^*$  may form the molecules with the spin-parity  $J^{P(C)} = 1^{+(\pm)}$  with  $I = 1, 0$ , as listed in Table I<sup>2</sup>. In the following, we simultaneously study the relatively long-range  $DD^*/D\bar{D}^*$  interactions by exchanging the light mesons. We focus on the light

pseudoscalar (P) meson  $\pi^-$  and vector (V) meson  $\rho/\omega$ -exchange potentials for the  $DD^*/D\bar{D}^*$ , while the  $\sigma$ - and  $\eta$ -contribution are neglected due to their tiny contributions [15, 55, 56]. The interactions are derived using the Lagrangians given in Refs. [15, 55] based on heavy quark symmetry. The  $DD^*$  and  $D\bar{D}^*$  interactions are related to each other using the charge conjugation.

The  $DD^*$  and  $D\bar{D}^*$  potentials by exchanging the light-meson under the isospin bases are summarized in Table I. The potentials  $V_\pi$ ,  $V_{\rho/\omega}^u$  and  $V_{\rho/\omega}^t$  are given in terms of three coupling constant  $g(D^*DP)$ ,  $\lambda(D^*DV)$ , and  $\beta(DDV/D^*D^*V)$ , respectively, as shown in the Appendix. The constant  $g = 0.57$  is determined from the strong decay width of  $D^* \rightarrow D\pi$  [1].

Subsequently, we determine the above  $DD^*/D\bar{D}^*$  interaction by fitting the experimental  $T_{cc}^+$  spectral function with the contributions from the  $D^0 D^{*+}$  and  $D^{*0} D^+$  channels. The inclusive production of the  $T_{cc}^+$  in the  $pp \rightarrow D^0(p_{D_1}) D^0(p_{D_2}) \pi^+(p_\pi) X$ , will be interpreted with two mechanisms, as depicted in Fig. 1. The amplitude reads

$$i\mathcal{M}_{pp \rightarrow DD\pi X} = \mathcal{A}_{pp \rightarrow DD^* X}^\mu \left\{ g_{\mu\alpha} - \frac{i}{(2\pi)^4} \int d^4 q_{D^*} G_{D^* \mu\nu}(q_{D^*}) G_D(p_{D_1} + p_{D_2} + p_\pi - q_{D^*}) T_\alpha^\nu(q_{D^*}, p_{D_1} + p_\pi) \right\} \\ \times G_{D^*}^{\alpha\beta}(p_{D_2} + p_\pi) (g p_{\pi,\beta}) + (p_{D_1} \rightarrow p_{D_2}), \quad (1)$$

where  $\mathcal{A}_{pp \rightarrow DD^* X}^\mu$  is the production vertex  $pp \rightarrow DD^* X$ . In the energy region close to the threshold, we consider the  $S$ -wave  $DD^*$  production contribution only. We have explored both the iso-vector and iso-scalar assignment for the  $\mathcal{A}$  with the production amplitudes satisfying  $\mathcal{A}_{pp \rightarrow D^+ D^{*0} X}^\mu = \pm \mathcal{A}_{pp \rightarrow D^0 D^{*+} X}^\mu$ , respectively. We are able to find a satisfactory fit to the experimental data only in the iso-scalar case. The  $G_H$  is the propagator of the heavy meson  $H$ . The  $DD^*$  scattering amplitude  $T(p_{D^*}, p'_{D^*}) \equiv \epsilon_\mu^*(p_{D^*}) T^{\mu\nu}(p_{D^*}, p'_{D^*}) \epsilon_\nu(p'_{D^*})$  with  $\epsilon$  the polarization vector, can be solved from the relativistic Lippmann-Schwinger equation [57–60],

$$T(\vec{p}_{D^*}, \vec{p}'_{D^*}; E) = \mathcal{V}(\vec{p}_{D^*}, \vec{p}'_{D^*}; E) + \int d\vec{q} \\ \times \frac{\mathcal{V}(\vec{p}_{D^*}, \vec{q}; E) T(\vec{q}, \vec{p}'_{D^*}; E)}{E - \sqrt{m_D^2 + q^2} - \sqrt{m_{D^*}^2 + q^2} + i\epsilon}. \quad (2)$$

In our calculation, the  $D^0 D^{*+}$  and  $D^+ D^{*0}$  are two independent channels. Thus the  $T$  and  $\mathcal{V}$ -matrix are both  $2 \times 2$  matrices. The effective potential  $\mathcal{V}$  is obtained with

the light-meson exchange potentials which incorporates a form factor to ensure regularization and convergence,

$$\mathcal{V} = \left( V_\pi + V_{\rho/\omega}^t + V_{\rho/\omega}^u \right) \left( \frac{\Lambda^2}{\Lambda^2 + p_f^2} \frac{\Lambda^2}{\Lambda^2 + p_i^2} \right)^2, \quad (3)$$

where  $\Lambda$  is the cut-off parameter. The introduction of the form factor can suppress the  $\delta$  potential from the one-pion-exchange.

## III. RESULTS

The cutoff reflects the composite structure of related hadrons and the off-shell effect. However, we expect the results to be insensitive to the specifics of hadronic structure or off-shell effects. We should check the cut-off dependence in a reasonable range, around 0.8 GeV to 1.2 GeV. Only adjusting the cutoff value impacts the  $T$ -matrix value due to its role in compensating part of the UV divergence contribution. Thus, we expect that the cutoff dependence should be effectively absorbed into the coupling constants  $\lambda$  and  $\beta$  by fitting the data. To confirm this, we perform the fitting procedures with three values  $\Lambda = 0.8, 1.0$ , and 1.2 GeV, respectively, to check the quality of the three fits and the uncertainty of the

<sup>2</sup> The wave functions presented in Table I are shown to systematically describe all possible resonances. We did all the calculations on a physical particle basis instead of the isospin eigenstates. Thus, our result is independent of isospin eigenstates.

TABLE I. The  $D^*D$  and  $DD^*$  interactions in the one-boson-exchange model in the isospin symmetry limit. To facilitate comparison, we have employed the potential forms ( $D^*D$  interactions) to express both  $D^*D$  and  $DD^*$  interactions, denoted as  $V_\phi^{u/t}$  where the subscript  $\phi$  may be  $\pi, \rho, \omega$ . The C-parity of the flavor wave functions (neutral system)  $[D\bar{D}^*] = \frac{1}{\sqrt{2}}(D\bar{D}^* - D^*\bar{D})$  and  $\{D\bar{D}^*\} = \frac{1}{\sqrt{2}}(D\bar{D}^* + D^*\bar{D})$  are even and odd, respectively, using the charge conjugation convention  $D^* \rightarrow -\bar{D}^*$  from Ref. [13].

	wave function	$I(J^{PC})$	$u$ - channel : $\pi$	$u$ - channel : $\rho/\omega$	$t$ - channel : $\rho/\omega$
$DD^*$	$\frac{1}{\sqrt{2}}(D^+D^{*0} - D^0D^{*+})$	$0(1^+) [T_{cc}^+]$	$\frac{3}{2}V_\pi$	$\frac{3}{2}V_\rho^u - \frac{1}{2}V_\omega^u$	$-\frac{3}{2}V_\rho^t + \frac{1}{2}V_\omega^t$
	$\frac{1}{\sqrt{2}}(D^+D^{*0} + D^0D^{*+})$	$1(1^+)$	$\frac{1}{2}V_\pi$	$\frac{1}{2}V_\rho^u + \frac{1}{2}V_\omega^u$	$\frac{1}{2}V_\rho^t + \frac{1}{2}V_\omega^t$
$DD^*$	$\frac{1}{\sqrt{2}}([D^+D^{*-}] + [D^0\bar{D}^{*0}])$	$0(1^{++})[X(3872)]$	$\frac{3}{2}V_\pi$	$-\frac{3}{2}V_\rho^u - \frac{1}{2}V_\omega^u$	$-\frac{3}{2}V_\rho^t - \frac{1}{2}V_\omega^t$
	$\frac{1}{\sqrt{2}}([D^+D^{*-}] - [D^0\bar{D}^{*0}])$	$1(1^{++})$	$-\frac{1}{2}V_\pi$	$\frac{1}{2}V_\rho^u - \frac{1}{2}V_\omega^u$	$\frac{1}{2}V_\rho^t - \frac{1}{2}V_\omega^t$
	$\frac{1}{\sqrt{2}}(\{D^+D^{*-}\} + \{D^0\bar{D}^{*0}\})$	$0(1^{+-})[h_c]$	$-\frac{3}{2}V_\pi$	$\frac{3}{2}V_\rho^u + \frac{1}{2}V_\omega^u$	$-\frac{3}{2}V_\rho^t - \frac{1}{2}V_\omega^t$
	$\frac{1}{\sqrt{2}}(\{D^+D^{*-}\} - \{D^0\bar{D}^{*0}\})$	$1(1^{+-}) [Z_c(3900)]$	$\frac{1}{2}V_\pi$	$-\frac{1}{2}V_\rho^u + \frac{1}{2}V_\omega^u$	$\frac{1}{2}V_\rho^t - \frac{1}{2}V_\omega^t$

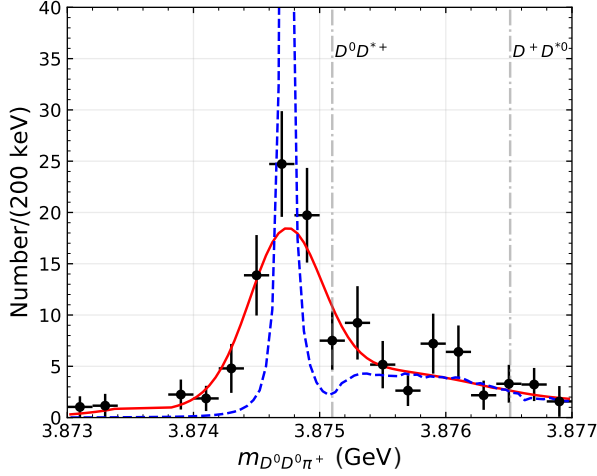


FIG. 2. (color online) The fitted lineshape of the  $T_{cc}^+$  in the  $D^0 D^0 \pi^+$  invariant mass spectrum [29]. The blue dashed and red solid lines represent the lineshapes before and after the convolution with the energy resolution function, which is taken from the LHCb collaboration [30].

attracted  $T_{cc}$  pole position. Indeed, our final results remain unchanged regardless of the chosen  $\Lambda$  value. When the cutoff  $\Lambda = 1.0$  GeV is taken, the fitted parameters are

$$\lambda = 0.683 \pm 0.025/\text{GeV}, \quad \beta = 0.687 \pm 0.017. \quad (4)$$

with  $\chi^2/\text{d.o.f.} = 0.78$ . The fitted line shape is shown in Fig. 2, together with the line shape before the convolution with the energy resolution function [30].

To identify  $T_{cc}^+$  and explore other possible resonant states while obtaining the wave function, we search the poles in the complex plane using  $T$ -matrix pole analysis and complex scaling method (CSM) [61–63], which is introduced in the Appendix. The results are consistent with each other on the bound and resonant states. Our

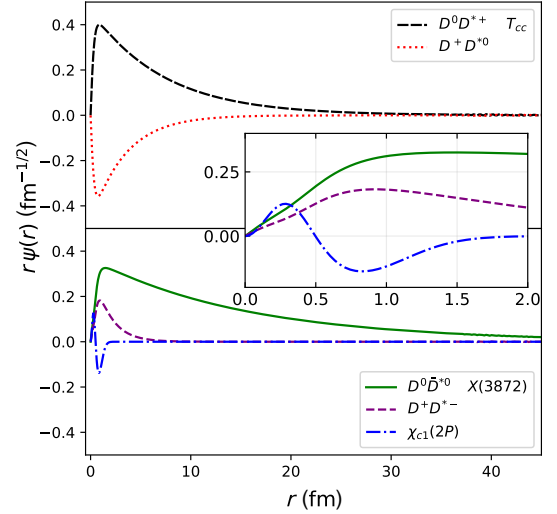


FIG. 3. (color online) The wave function distribution of different components for the  $T_{cc}^+$  and  $X(3872)$ .

results clearly show a distinct signal corresponding to the bound state of the  $DD^*$ . We summarize its properties including the mass, decay width, root mean square radius and proportions of different components in Table II. The binding energy of the bound state is  $\Delta E = -393.0$  keV, which is consistent with that of the experiment  $\Delta E_{\text{exp}} = -360(40)$  keV [30]. In our model, the whole calculation is conducted in the momentum space and the on-shell contribution is included, which naturally generates the width of the  $T_{cc}^+$  around 70 keV through the decay into the  $DD\pi$  final state. In Ref. [44], the  $D^*$  width in the intermediate loops was found to have non-negligible contribution to the  $T_{cc}^+$  width. In our present calculation, the width of  $D^*$  is not included since our ba-

sic model focuses on the two-body system, rather than  $\pi DD$  system. The impact of the three-body effects will be studies in the future under the same framework.

The wave function of  $T_{cc}^+$  is presented in Fig. 3. As a shallow S-wave bound state, there is a long tail for the radius distribution. The root mean square radius is around 4.7 fm which establishes the  $T_{cc}^+$  as a molecular state of the  $DD^*$ . The ratio of the residue of the  $D^{*+}D^0$  and  $D^+D^{*0}$  channels is close to 1, showing the similar couplings of the  $T_{cc}^+$  to these two components. Then the difference between the wave functions of two channels is mainly due to their mass difference of 1.4 MeV. Such small mass splitting still introduces a sizeable isospin breaking effect because of its extremely small binding energy, and the iso-vector component occupies around 4.2% in  $T_{cc}^+$  as shown in Table II.

The successful interpretation of the  $T_{cc}^+$  encourages us to study the molecular states in the  $DD^*$  sector composed of the  $\bar{D}^0D^{*0}$  and  $D^+D^{*-}$ . With the  $DD^*$  interactions, we derive the  $DD^*$  interactions through the charge conjugation. Then in the  $J^{PC} = 1^{++}$  sector where the  $X(3872)$  exists, we do not find any bound state, but we obtain a virtual state with  $E_v = 3870.0 + 0.26i$  MeV in the second Riemann sheet of the neutral channel and the first Riemann sheet of the charged channel. Interestingly, if we introduce a scaling factor ( $> 1$ ), for example 1.15, to all couplings of the  $D^*\bar{D}$  potentials, a bound state appears with a binding energy  $-25$  keV. This indicates that the  $DD^*$  interaction is attractive but not strong enough to produce a bound state. The conclusion remains the same using the different cut off value such as 0.8 or 1.2 GeV. Moreover, the bound state can be obtained by fine-tuning the coupling strength in the OBE model as shown above. Therefore the constraint from the  $T_{cc}^+$  is indispensable to study the formation mechanism of the  $X(3872)$ .

In fact, the  $DD^*$  system with the quantum numbers  $I(J^{PC}) = 0(1^{++})$  can couple with the  $\chi_{c1}(2P)$ . In the following, we demonstrate that the inclusion of the bare  $c\bar{c}$  core is essential to form the  $X(3872)$ . The mass and wave functions of  $\chi_{c1}(2P)$  are determined by using the GI model with the updated parameters from our previous works [64, 65]. To account for the coupled channel effect between the  $c\bar{c}$  core and  $DD^{(*)}$ , we employ the quark-pair-creation (QPC) model. Within the framework, a light quark pair with the spin-parity  $J^{PC} = 0^{++}$  is created and combined with the  $c\bar{c}$  pair to form the  $DD^*$  state. This approach provides a feasible connection between the quark and hadron level. The transition potential reads [66–72],

$$g_{D\bar{D}^*,c\bar{c}}(|\vec{k}_{D\bar{D}^*}|) = \gamma I_{D\bar{D}^*,c\bar{c}}(|\vec{k}_{D\bar{D}^*}|), \quad (5)$$

where  $\vec{k}_{D\bar{D}^*}$  is the relative momentum in the  $DD^*$  channel.  $I_{D\bar{D}^*,c\bar{c}}(|\vec{k}_{D\bar{D}^*}|)$  is the overlap of the meson wave functions. The parameter  $\gamma$  represents the amplitude of producing the light quark pair. We choose  $\gamma = 4.69$  so that it reproduces the mass and decay of  $\psi(3770)(\rightarrow DD)$

resonance. There may be additional contributions for the  $DD^*$  interactions, such as the exchange of heavy mesons and their excitations, leading to the coupling  $DD^* - \text{charmonium} + \text{light mesons}$ . In the molecular scenario, such contributions to the  $DD^*$  rescattering effects are significantly suppressed compared with those originating from the  $DD^* - c\bar{c}$  coupling and not included in this work.

Using the CSM method, our results show a clear signal of a bound state associated with the  $X(3872)$  with a binding energy  $\Delta E = -80.4$  keV and a resonant state corresponding to a dressed  $c\bar{c}$  state with  $J^{PC} = 1^{++}$ .

In Table II, we summarize the properties of  $X(3872)$ . Its width, 32.5 keV, arises predominantly from the decay into the  $D^0\bar{D}^0\pi^0$  channel. The dominant component of the  $X(3872)$  is the loosely bound molecular state of the neutral  $D^0\bar{D}^{*0}$  (94.0%) and charged  $D^+\bar{D}^{*-}$  (4.8%). The mass difference of 8 MeV between the charged and neutral channels leads to an important isospin breaking for a bound state extremely close to the neutral channel. It is worth highlighting that the  $c\bar{c}$  component is crucial to form the  $X(3872)$ , even though it only accounts for 1.2%.

To visualize the contribution of the  $c\bar{c}$ ,  $D^+D^{*-}$  and  $D^0\bar{D}^{*0}$  components in the  $X(3872)$ , we display their wave functions in the lower and middle panels of Fig. 3. We employ the  $c\bar{c}$  wave function from the GI model, combining with its probability amplitude in the  $X(3872)$ . In the short-range region up to 2 fm (middle panel of Fig. 3), both the  $c\bar{c}$  and  $DD^*$  components are significant. Notably, for  $r < 0.5$  fm, the  $c\bar{c}$  core dominates. The wave functions show that the main component  $DD^*$  definitely plays the dominant role in the long-distance region, which contributes to the large size of the  $X(3872)$  whose radius around 11.2 fm. This is reasonable because the  $X(3872)$  has such a tiny binding energy and couples strongly with the  $DD^*$  channel.

The isospin-breaking decays  $X(3872) \rightarrow J/\psi\omega/\rho$  is attributed to the overlap factor of the wave functions  $\int d\vec{p} \psi_{X(3872)}^{I=1/0}(\vec{p}) \psi_{J/\psi}^*(\vec{p})$  in the amplitude [16], yielding a ratio  $R_{\omega/\rho} = \frac{\mathcal{B}[X \rightarrow J/\psi\omega]}{\mathcal{B}[X \rightarrow J/\psi\rho]} = 21.4$ . Using the factorization formulae [73–75], the decay ratio  $\frac{\mathcal{B}[X \rightarrow J/\psi\pi^+\pi^-\pi^0]}{\mathcal{B}[X \rightarrow J/\psi\pi^+\pi^-]} = R_{\omega/\rho} \times R_2$  is 1.86 and 3.14, with  $R_2 \sim \frac{\mathcal{B}(\omega \rightarrow \pi^+\pi^-\pi^0)}{\mathcal{B}(\rho \rightarrow \pi^+\pi^-)}$  being 0.087 [73] and 0.147 [74, 75], respectively. The former decay ratio is consistent with the experimental value  $1.0 \pm 0.4 \pm 0.3$  [76]. Besides the  $X(3872)$ , we also find a signal of the resonant state  $\chi_{c1}(2P)$  at

$$M = 3957.9 \text{ MeV}, \quad \Gamma = 16.7 \text{ MeV}, \quad (6)$$

which might be identified as the  $X(3940)(M = 3942 \pm 9 \text{ MeV}$  and  $\Gamma = 37_{-17}^{+27} \text{ MeV})$  observed in the  $DD^*$  channel [77].

Moreover, in the  $J^{PC} = 1^{+-}$  sector, we investigate the coupling between the  $h_c(2P)$  component and iso-scalar  $DD^*$  channel. Two poles are observed. One is a virtual state around  $M = 3870.2$  MeV. Since the  $t$ -channel vec-



TABLE II. The properties of the  $T_{cc}^+$  and  $X(3872)$  in the fit with  $\Lambda = 1.0$  GeV. The script “BE” denotes the binding energy. The ratio of the residue in two channels is listed in the last column. For  $X(3872)$ , the QPC parameter  $\gamma = 4.69$ .

	BE (keV)	$\Gamma$ (keV)	$\sqrt{\langle r^2 \rangle}$	$I = 0$	$I = 1$	$P(D^0 D^{*+})$	$P(D^+ D^{*0})$	$ \frac{\text{Res}(D^0 D^{*+})}{\text{Res}(D^+ D^{*0})} $
$T_{cc}^+$	-393.0	70.4	4.7 fm	95.8%	4.2%	70.0%	30.0%	1.055
	BE (keV)	$\Gamma$ (keV)	$\sqrt{\langle r^2 \rangle}$	$I = 0$	$I = 1$	$P(D^0 \bar{D}^{*0})$	$P(D^+ \bar{D}^{*-})$	$P(c\bar{c})$
$X(3872)$	-80.4	32.5	11.2 fm	71.9%	28.1%	94.0%	4.8%	1.2%

tor meson exchange potentials dominate, it is related to an isoscalar state  $X(3872)$  with a mass  $3860.0 \pm 10.4$  MeV discovered by COMPASS Collaboration [78]. The existence of  $\tilde{X}(3872)$  is also post-predicted by several theoretical investigations [79–81]. Another signal corresponds to the excited  $h_c(2P)$  whose pole is around  $M = 3961.3$  MeV with the width  $\Gamma = 1.1$  MeV.

#### IV. DISCUSSION AND CONCLUSION

In this work, we first analyze the  $DD\pi$  invariant mass distributions for the  $T_{cc}^+$  in the molecular scenario using a coupled-channel formalism. We derived the scattering potential involving the light mesons ( $\pi$ ,  $\rho$ ,  $\omega$ ) from a heavy hadron effective Lagrangian. The data can be well described. The one-boson-exchange  $DD^*$  potentials enable a direct connection to the  $D\bar{D}^*$  potentials via the charge conjugation symmetry. Thus, we set up a universal framework for the  $DD^*/D\bar{D}^*$  molecules. It is different from the other frameworks which have the contact constant potentials. Although they can well fit the experimental data, all the dynamical information is encoded in the parameters. Notably, the short-range interactions in the  $D\bar{D}^*$  and  $DD^*$  are distinct due to the potential annihilation of the light and heavy quark-antiquark pair in the  $D\bar{D}^*$  system. As a result, the direct application of charge conjugation symmetry to derive the contact potentials for the  $D\bar{D}^*$  from the  $DD^*$  sector is not feasible. In our framework, the differences of the short-range interaction of  $D\bar{D}^*$  and  $DD^*$  mainly arises from the significant role of the charmonium state which couples with the  $D\bar{D}^*$ . This assumption promises that the OBE model can be fairly applied in both sectors through the charge conjugation symmetry.

Within our framework, we explore two fine-tuning mechanisms of the  $X(3872)$ . Our results show that the pure  $D\bar{D}^*$  interaction is attractive but insufficient to form a bound state  $X(3872)$ . The P-wave  $c\bar{c}$  core plays a crucial role in the formation of the  $X(3872)$ , even though its proportion is quite small. Notably, the wave function of the  $X(3872)$  shows that the  $D\bar{D}^*$  component has a long tail causing its large radius, while the  $c\bar{c}$  is significant at short distances. Furthermore, our study successfully identifies three clear signals related to the  $\tilde{X}(3872)$ ,  $X(3940)$ , and  $h_c(2P)$  states. The  $X(3940)$  which was first observed in  $D\bar{D}^*$  channel awaits further exploration,

and the  $h_c(2P)$  state remains to be discovered. These findings can serve as benchmarks for evaluating our new model in future experiments.

Notably, this framework can be extended to establish other exotic states, for which no consensus has been reached for their dynamic origins. They often exhibit characteristics that come from the mixing of various dynamic sources. Therefore, it is important and useful to identify and study their dynamics from their relations to the well-understood hadronic states. Such a systematic approach may allow us to unravel the intricate structure of the exotic hadronic states, providing a unique and reliable pathway for investigating the  $XYZ$  particles.

#### ACKNOWLEDGMENTS

We thank useful discussions and valuable comments from Dote Akinobu, Meng-Lin Du, Jian-Bo Cheng, Rui Chen, Feng-Kun Guo, Zi-Yang Lin, Lu Meng, Mao-Jun Yan, Bing-Song Zou. This work is partly supported by the KAKENHI under Grant Nos. 19H05159, 20K03959, and 21H00132 (M.O.), and 23K03427 (M.O. and G.J.W), and by the National Natural Science Foundation of China (NSFC) under Grants Nos. 12275046 (Z.Y.), 12175239 and 12221005 (J.J.W), 11975033 and 12070131001 (S.L.Z.), and by the Natural Science Foundation of Sichuan Province under Grant No. 2022NS-FSC1795 (Z.Y.), and by the National Key R&D Program of China under Contract No. 2020YFA0406400 (J.J.W), and by the Chinese Academy of Sciences under Grant No. YSBR-101 (J.J.W).

#### Author contributions:

Jia-Jun Wu proposed the main idea in this project. Guang-Juan Wang and Zhi Yang did the calculations and drafted the manuscript. Makoto Oka and Shi-Lin Zhu refined the idea and checked the results. All the authors made substantial contributions to the discussions and the editing of the manuscript. All the authors have approved the final version of this manuscript.

## Appendix A: Fit details

The differential cross section for the  $pp \rightarrow D(p_{D_1})D(p_{D_2})\pi(p_\pi)$  channel reads

$$\begin{aligned} d\sigma_{pp \rightarrow XDD\pi} &= \frac{(2\pi)^4}{4\sqrt{(p_{p_1} \cdot p_{p_2} - m_p^2 m_p^2)}} |\mathcal{M}|^2 d\Phi_{XDD\pi} \\ \frac{d\sigma_{pp \rightarrow XDD\pi}}{dm_{DD\pi}} &\approx 2m_{DD\pi} \int d\sigma_{pp \rightarrow X+DD\pi} B_2 d\Phi_{DD\pi} \\ &\approx 2m_{DD\pi} \int dm_{12} dm_{23} B_2(E; m_{12}, m_{23}), \end{aligned} \quad (\text{A1})$$

where  $p_{p_1}$  ( $p_{p_2}$ ) and  $m_p$  are the momentum and mass of the initial photon.  $m_{ij}$  is defined as  $m_{ij}^2 = (p_i + p_j)^2$  with  $p_i$  the momutum of  $D$  or  $\pi$  in the final state.  $B_2$  is obtained with the  $\mathcal{M}$ ,

$$\begin{aligned} |\mathcal{M}|^2 &= |a_{pp \rightarrow DD^*X}|^2 B_2, \\ B_2 &= \sum_{\lambda_X} \epsilon_\mu(p_X, \lambda_X) \epsilon_{\mu'}^\dagger(p_X, \lambda_X) \mathcal{B}_\mu \mathcal{B}^{\dagger\mu'}. \end{aligned} \quad (\text{A2})$$

To obtain Eq. (A1) in the energy region close to the threshold, we have approximated  $\mathcal{A}_{pp \rightarrow DD^*X}^\mu = a_{pp \rightarrow DD^*X} \epsilon^\mu(p_X, \lambda_X)$  with  $a_{pp \rightarrow DD^*X}$  a constant and independent of the polarization. Moreover, the scattering cross section  $\sigma_{pp \rightarrow X+DD\pi}$  is a constant since we only concentrate on a small energy range. For a specific channel, the  $\mathcal{B}_j^\mu$  (the  $j$ -th represents the  $D^*D$  channels) reads

$$\begin{aligned} \mathcal{B}_j^\mu(p_{12}, p_{23}) &= g \left\{ \frac{-i(p_\pi^\mu - \frac{p_{12}^\mu p_{12} \cdot p_\pi}{m_{D^*}^2})}{p_{12}^2 - m_{D^*}^2 + im_{D^*} \Gamma_{D^*}} \right\}_j + \sum_{i=1,2} ig \int dq_{D^*} q_{D^*}^2 \frac{d\Omega_{q_{D^*}}}{4\pi} \frac{\sqrt{2w_{D_2}}}{\sqrt{2w_{D^*}}} \frac{\sqrt{2w_{D_{12}^*}}}{\sqrt{2w_D}} \\ &\times \frac{T_{ij}^{J00}(M, |q_{D^*}|, |p_{12}|)}{(M - w_{D^*}^i) - w_D^i + i\epsilon} \left\{ \frac{\epsilon_a^{*\mu}(w_{D^*}, q_{D^*}) \epsilon_a(p_{12}) \cdot p_\pi}{p_{12}^2 - m_{D^*}^2 + im_{D^*} \Gamma_{D^*}} \right\}_j + (p_{D_1} \rightarrow p_{D_2}). \end{aligned} \quad (\text{A3})$$

where the notations are  $p_{12} = p_{D_1} + p_\pi$ ,  $p_{23} = p_{D_2} + p_\pi$  and  $w_H = m_H^2 + p_H^2$ . In the  $DD^*$  scattering, we only consider the S-wave contribution. The  $T_{i1}^{J00}$  is derived after the partial wave decomposition of the  $T(\vec{k}_{D^*}, \vec{k}_{D^*}; E)$ .

The explicit forms of the potentials in constructing the  $T$ -matrix read

$$V_\pi = \frac{g^2 (q \cdot \epsilon_\lambda) (q \cdot \epsilon_{\lambda'}^\dagger)}{f_\pi^2 (q^2 - m_\pi^2)}, \quad (\text{A4})$$

$$V_{\rho/\omega}^u = -2\lambda^2 g_V^2 \frac{(\epsilon_{\lambda'}^\dagger \cdot q)(\epsilon_\lambda \cdot q) - q^2 (\epsilon_\lambda \cdot \epsilon_{\lambda'}^\dagger)}{q^2 - m_{\rho/\omega}^2}, \quad (\text{A5})$$

$$V_{\rho/\omega}^t = \frac{\beta^2 g_V^2 (\epsilon_\lambda \cdot \epsilon_{\lambda'}^\dagger)}{2 (q^2 - m_{\rho/\omega}^2)}. \quad (\text{A6})$$

Here we introduce a constant  $g_V = 5.8$  to compare our parameters with other values from the phenomenological estimation [15, 55, 56].

## Appendix B: The Independence of the cut-off $\Lambda$

Besides the values  $\Lambda = 1.0$  GeV, we also used other two different values 0.8 and 1.2 GeV for  $\Lambda$ . The lineshapes fitted with  $\Lambda = 0.8$  and 1.2 GeV are shown in Fig. 4. As one can see the obtained results are almost the same. The fitting parameters are

$$\begin{aligned} \lambda_{\Lambda=0.8} &= 0.890/\text{GeV}, \quad \beta_{\Lambda=0.8} = 0.810; \\ \lambda_{\Lambda=1.2} &= 0.587/\text{GeV}, \quad \beta_{\Lambda=1.2} = 0.550. \end{aligned} \quad (\text{B1})$$

The properties of the  $T_{cc}^+$  with the fitting parameters are summarized in Table III, which clearly shows the independence of the results on the values of the cutoff  $\Lambda$ .

## Appendix C: Complex scaling method

The complex scaling method (CSM) is used to identify the bound and resonant states. In CSM, the radius and momentum will rotate with an angle  $\theta$ ,  $\mathbf{r} \rightarrow \mathbf{r}e^{i\theta}$ ,  $\mathbf{q} \rightarrow \mathbf{q}e^{-i\theta}$ . With the varying  $\theta$ , the scattering states will rotate with  $2\theta$ , while the bound and resonant states are independent of the  $\theta$  and will stay stable. More technical details can be found in Refs. [61–63]. The complex eigenvalues for the  $DD^*$  system ( $T_{cc}$ ), the  $D\bar{D}^{(*)}$  system with  $J^{PC} = 1^{--}$  ( $\psi(3770)$ ), and  $D\bar{D}^*$  system  $J^{PC} = 1^{++}$  ( $X(3872)$ ) with the fixed cutoff  $\Lambda = 1.0$  GeV are displayed Fig. 5.

TABLE III. The properties of the  $T_{cc}^+$  [29] in the three fits with the cutoff values  $\Lambda = 0.8, 1.0$ , and  $1.2$  GeV. The script “BE” denotes the binding energy. The ratio of the residue in two channels is listed in the last column.

$\Lambda$ (GeV)	BE (keV)	$\Gamma$ (keV)	$\sqrt{\langle r^2 \rangle}$	$I = 0$	$I = 1$	$P(D^0 D^{*+})$	$P(D^+ D^{*0})$	$\frac{\text{Res}(D^0 D^{*+})}{\text{Res}(D^+ D^{*0})}$
0.8	-387.7	67.3	4.8 fm	95.8%	4.2%	70.0%	30.0%	$-1.063 + 0.001I$
1.0	-393.0	70.4	4.7 fm	95.8%	4.2%	70.0%	30.0%	$-1.055 + 0.001I$
1.2	-391.6	72.7	4.7 fm	95.7%	4.3%	70.3%	29.7%	$-1.052 + 0.001I$

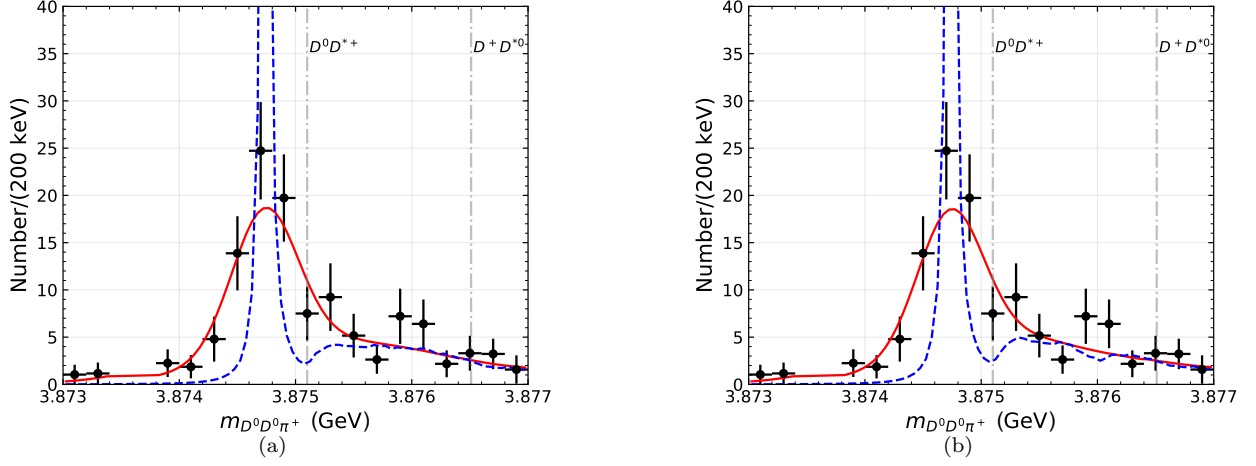


FIG. 4. (color online) The fitting results by employing the light-meson-exchanging potential with the cutoff (a)  $\Lambda = 0.8$  GeV, (b)  $1.2$  GeV. The  $\chi^2/\text{d.o.f.}$  are 0.76 and 0.78, respectively.

- [1] R. L. Workman et al. (Particle Data Group), Review of Particle Physics, *PTEP* **2022**, 083C01 (2022).
- [2] S. K. Choi et al. (Belle), Observation of a narrow charmonium-like state in exclusive  $B^\pm \rightarrow K^\pm \pi^+ \pi^- J/\psi$  decays, *Phys. Rev. Lett.* **91**, 262001 (2003), [arXiv:hep-ex/0309032](#).
- [3] D. Acosta et al. (CDF), Observation of the narrow state  $X(3872) \rightarrow J/\psi \pi^+ \pi^-$  in  $p\bar{p}$  collisions at  $\sqrt{s} = 1.96$  TeV, *Phys. Rev. Lett.* **93**, 072001 (2004), [arXiv:hep-ex/0312021](#).
- [4] V. M. Abazov et al. (D0), Observation and properties of the  $X(3872)$  decaying to  $J/\psi \pi^+ \pi^-$  in  $p\bar{p}$  collisions at  $\sqrt{s} = 1.96$  TeV, *Phys. Rev. Lett.* **93**, 162002 (2004), [arXiv:hep-ex/0405004](#).
- [5] B. Aubert et al. (BaBar), Study of the  $B \rightarrow J/\psi K^- \pi^+ \pi^-$  decay and measurement of the  $B \rightarrow X(3872) K^-$  branching fraction, *Phys. Rev. D* **71**, 071103 (2005), [arXiv:hep-ex/0406022](#).
- [6] R. Aaij et al. (LHCb), Observation of  $X(3872)$  production in  $pp$  collisions at  $\sqrt{s} = 7$  TeV, *Eur. Phys. J. C* **72**, 1972 (2012), [arXiv:1112.5310 \[hep-ex\]](#).
- [7] R. Aaij et al. (LHCb), Determination of the  $X(3872)$  meson quantum numbers, *Phys. Rev. Lett.* **110**, 222001 (2013), [arXiv:1302.6269 \[hep-ex\]](#).
- [8] S. Chatrchyan et al. (CMS), Measurement of the  $X(3872)$  Production Cross Section Via Decays to  $J/\psi \pi^+ \pi^-$  in  $pp$  collisions at  $\sqrt{s} = 7$  TeV, *JHEP* **04**, 154, [arXiv:1302.3968 \[hep-ex\]](#).
- [9] S. Godfrey and N. Isgur, Mesons in a Relativized Quark Model with Chromodynamics, *Phys. Rev. D* **32**, 189 (1985).
- [10] T. Barnes and S. Godfrey, Charmonium options for the  $X(3872)$ , *Phys. Rev. D* **69**, 054008 (2004), [arXiv:hep-ph/0311162](#).
- [11] Y. S. Kalashnikova and A. V. Nefediev,  $X(3872)$  as a  $^1D_2$  charmonium state, *Phys. Rev. D* **82**, 097502 (2010), [arXiv:1008.2895 \[hep-ph\]](#).
- [12] N. A. Tornqvist, Isospin breaking of the narrow charmonium state of Belle at 3872 MeV as a deuson, *Phys. Lett. B* **590**, 209 (2004), [arXiv:hep-ph/0402237](#).
- [13] Y.-R. Liu, X. Liu, W.-Z. Deng, and S.-L. Zhu, Is  $X(3872)$  Really a Molecular State?, *Eur. Phys. J. C* **56**, 63 (2008), [arXiv:0801.3540 \[hep-ph\]](#).
- [14] X. Liu, Z.-G. Luo, Y.-R. Liu, and S.-L. Zhu,  $X(3872)$  and Other Possible Heavy Molecular States, *Eur. Phys. J. C* **61**, 411 (2009), [arXiv:0808.0073 \[hep-ph\]](#).
- [15] N. Li and S.-L. Zhu, Isospin breaking, Coupled-channel effects and Diagnosis of  $X(3872)$ , *Phys. Rev. D* **86**, 074022 (2012), [arXiv:1207.3954 \[hep-ph\]](#).
- [16] E. Braaten and M. Kusunoki, Low-energy universality and the new charmonium resonance at 3870 MeV, *Phys. Rev. D* **69**, 074005 (2004), [arXiv:hep-ph/0311147](#).
- [17] Y. S. Kalashnikova, Coupled-channel model for charmonium levels and an option for  $X(3872)$ , *Phys. Rev. D* **72**,

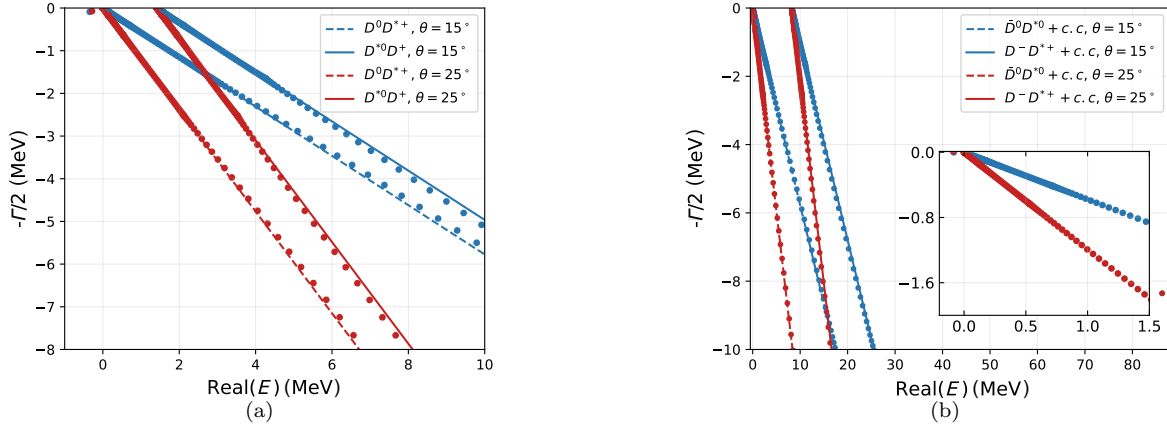


FIG. 5. (color online) The complex eigenvalues by employing the light-meson-exchanging potential with the cutoff  $\Lambda = 1.0$  GeV in the channels: (a)  $D^0 D^{*+}$  and  $D^{*0} D^+$  channels; (b)  $\chi_{c1}(2P)$ ,  $\bar{D}^0 D^{*0}$  and  $D^- D^{*+}$  channels. The bound states in (a) and (b) correspond to the  $T_{cc}^+$  and  $X(3872)$ , respectively. The resonant state in (b) is related to the  $X(3940)$ . The y-axis of the eigenvalues in CSM method corresponds to the half of the decay width.

- 034010 (2005), [arXiv:hep-ph/0506270](#).
- [18] T. Barnes and E. S. Swanson, Hadron loops: General theorems and application to charmonium, *Phys. Rev. C* **77**, 055206 (2008), [arXiv:0711.2080 \[hep-ph\]](#).
- [19] P. G. Ortega, J. Segovia, D. R. Entem, and F. Fernandez, Coupled channel approach to the structure of the  $X(3872)$ , *Phys. Rev. D* **81**, 054023 (2010), [arXiv:0907.3997 \[hep-ph\]](#).
- [20] B.-Q. Li, C. Meng, and K.-T. Chao, Coupled-Channel and Screening Effects in Charmonium Spectrum, *Phys. Rev. D* **80**, 014012 (2009), [arXiv:0904.4068 \[hep-ph\]](#).
- [21] V. Baru, C. Hanhart, Y. S. Kalashnikova, A. E. Kudryavtsev, and A. V. Nefediev, Interplay of quark and meson degrees of freedom in a near-threshold resonance, *Eur. Phys. J. A* **44**, 93 (2010), [arXiv:1001.0369 \[hep-ph\]](#).
- [22] E. Cincioglu, J. Nieves, A. Ozpineci, and A. U. Yilmazer, Quarkonium Contribution to Meson Molecules, *Eur. Phys. J. C* **76**, 576 (2016), [arXiv:1606.03239 \[hep-ph\]](#).
- [23] Y. Yamaguchi, A. Hosaka, S. Takeuchi, and M. Takizawa, Heavy hadronic molecules with pion exchange and quark core couplings: a guide for practitioners, *J. Phys. G* **47**, 053001 (2020), [arXiv:1908.08790 \[hep-ph\]](#).
- [24] H.-X. Chen, W. Chen, X. Liu, and S.-L. Zhu, The hidden-charm pentaquark and tetraquark states, *Phys. Rept.* **639**, 1 (2016), [arXiv:1601.02092 \[hep-ph\]](#).
- [25] A. Esposito, A. Pilloni, and A. D. Polosa, Multiquark Resonances, *Phys. Rept.* **668**, 1 (2017), [arXiv:1611.07920 \[hep-ph\]](#).
- [26] N. Brambilla, S. Eidelman, C. Hanhart, A. Nefediev, C.-P. Shen, C. E. Thomas, A. Vairo, and C.-Z. Yuan, The  $XYZ$  states: experimental and theoretical status and perspectives, *Phys. Rept.* **873**, 1 (2020), [arXiv:1907.07583 \[hep-ex\]](#).
- [27] Y. S. Kalashnikova and A. V. Nefediev,  $X(3872)$  in the molecular model, *Phys. Usp.* **62**, 568 (2019), [arXiv:1811.01324 \[hep-ph\]](#).
- [28] T.-W. Wu, Y.-W. Pan, M.-Z. Liu, and L.-S. Geng, Multi-hadron molecules: status and prospect, *Sci. Bull.* **67**, 1735 (2022), [arXiv:2208.00882 \[hep-ph\]](#).
- [29] R. Aaij et al. (LHCb), Observation of an exotic narrow doubly charmed tetraquark, *Nature Phys.* **18**, 751 (2022), [arXiv:2109.01038 \[hep-ex\]](#).
- [30] R. Aaij et al. (LHCb), Study of the doubly charmed tetraquark  $T_{cc}^+$ , *Nature Commun.* **13**, 3351 (2022), [arXiv:2109.01056 \[hep-ex\]](#).
- [31] S. S. Agaev, K. Azizi, and H. Sundu, Newly observed exotic doubly charmed meson  $T_{cc}^+$ , *Nucl. Phys. B* **975**, 115650 (2022), [arXiv:2108.00188 \[hep-ph\]](#).
- [32] X.-Z. Ling, M.-Z. Liu, L.-S. Geng, E. Wang, and J.-J. Xie, Can we understand the decay width of the  $T_{cc}^+$  state?, *Phys. Lett. B* **826**, 136897 (2022), [arXiv:2108.00947 \[hep-ph\]](#).
- [33] R. Chen, Q. Huang, X. Liu, and S.-L. Zhu, Predicting another doubly charmed molecular resonance  $T_{cc}^+$  (3876), *Phys. Rev. D* **104**, 114042 (2021), [arXiv:2108.01911 \[hep-ph\]](#).
- [34] X.-K. Dong, F.-K. Guo, and B.-S. Zou, A survey of heavy-heavy hadronic molecules, *Commun. Theor. Phys.* **73**, 125201 (2021), [arXiv:2108.02673 \[hep-ph\]](#).
- [35] A. Feijoo, W. H. Liang, and E. Oset,  $D^0 D^0 \pi^+$  mass distribution in the production of the  $T_{cc}$  exotic state, *Phys. Rev. D* **104**, 114015 (2021), [arXiv:2108.02730 \[hep-ph\]](#).
- [36] M.-J. Yan and M. P. Valderrama, Subleading contributions to the decay width of the  $T_{cc}^+$  tetraquark, *Phys. Rev. D* **105**, 014007 (2022), [arXiv:2108.04785 \[hep-ph\]](#).
- [37] Q. Xin and Z.-G. Wang, Analysis of the doubly-charmed tetraquark molecular states with the QCD sum rules, *Eur. Phys. J. A* **58**, 110 (2022), [arXiv:2108.12597 \[hep-ph\]](#).
- [38] Y. Huang, H. Q. Zhu, L.-S. Geng, and R. Wang, Production of  $T_{cc}^+$  exotic state in the  $\gamma p \rightarrow D^+ T_{cc}^+ \Lambda_c^+$  reaction, *Phys. Rev. D* **104**, 116008 (2021), [arXiv:2108.13028 \[hep-ph\]](#).



- [39] S. Fleming, R. Hodges, and T. Mehen,  $T_{cc}^+$  decays: Differential spectra and two-body final states, *Phys. Rev. D* **104**, 116010 (2021), [arXiv:2109.02188 \[hep-ph\]](#).
- [40] K. Azizi and U. Özdem, Magnetic dipole moments of the  $T_{cc}^+$  and  $Z_V^{++}$  tetraquark states, *Phys. Rev. D* **104**, 114002 (2021), [arXiv:2109.02390 \[hep-ph\]](#).
- [41] Y. Hu, J. Liao, E. Wang, Q. Wang, H. Xing, and H. Zhang, Production of doubly charmed exotic hadrons in heavy ion collisions, *Phys. Rev. D* **104**, L111502 (2021), [arXiv:2109.07733 \[hep-ph\]](#).
- [42] K. Chen, R. Chen, L. Meng, B. Wang, and S.-L. Zhu, Systematics of the heavy flavor hadronic molecules, *Eur. Phys. J. C* **82**, 581 (2022), [arXiv:2109.13057 \[hep-ph\]](#).
- [43] M. Albaladejo, Tcc+ coupled channel analysis and predictions, *Phys. Lett. B* **829**, 137052 (2022), [arXiv:2110.02944 \[hep-ph\]](#).
- [44] M.-L. Du, V. Baru, X.-K. Dong, A. Filin, F.-K. Guo, C. Hanhart, A. Nefediev, J. Nieves, and Q. Wang, Coupled-channel approach to Tcc+ including three-body effects, *Phys. Rev. D* **105**, 014024 (2022), [arXiv:2110.13765 \[hep-ph\]](#).
- [45] C. Deng and S.-L. Zhu,  $T_{cc}^+$  and its partners, *Phys. Rev. D* **105**, 054015 (2022), [arXiv:2112.12472 \[hep-ph\]](#).
- [46] S. S. Agaev, K. Azizi, and H. Sundu, Hadronic molecule model for the doubly charmed state  $T_{cc}^+$ , *JHEP* **06**, 057, [arXiv:2201.02788 \[hep-ph\]](#).
- [47] E. Braaten, L.-P. He, K. Ingles, and J. Jiang, Triangle singularity in the production of Tcc+(3875) and a soft pion, *Phys. Rev. D* **106**, 034033 (2022), [arXiv:2202.03900 \[hep-ph\]](#).
- [48] J. He and X. Liu, The quasi-fission phenomenon of double charm  $T_{cc}^+$  induced by nucleon, *Eur. Phys. J. C* **82**, 387 (2022), [arXiv:2202.07248 \[hep-ph\]](#).
- [49] L. M. Abreu, H. P. L. Vieira, and F. S. Navarra, Multiplicity of the doubly charmed state Tcc+ in heavy-ion collisions, *Phys. Rev. D* **105**, 116029 (2022), [arXiv:2202.10882 \[hep-ph\]](#).
- [50] N. N. Achasov and G. N. Shestakov, Triangle singularities in the  $T_{cc} \rightarrow D^* + D^0 \rightarrow \pi + D^0 D^0$  decay width, *Phys. Rev. D* **105**, 096038 (2022), [arXiv:2203.17100 \[hep-ph\]](#).
- [51] M. Mikhasenko, Effective-range expansion of the  $T_{cc}^+$  state at the complex  $D^{*+}D^0$  threshold, (2022), [arXiv:2203.04622 \[hep-ph\]](#).
- [52] B. Wang and L. Meng, Revisiting the DD\* chiral interactions with the local momentum-space regularization up to the third order and the nature of Tcc+, *Phys. Rev. D* **107**, 094002 (2023), [arXiv:2212.08447 \[hep-ph\]](#).
- [53] C.-R. Deng and S.-L. Zhu, Decoding the double heavy tetraquark state  $T_{cc}^+$ , *Sci. Bull.* **67**, 1522 (2022), [arXiv:2204.11079 \[hep-ph\]](#).
- [54] Y. Lyu, S. Aoki, T. Doi, T. Hatsuda, Y. Ikeda, and J. Meng, Doubly Charmed Tetraquark Tcc+ from Lattice QCD near Physical Point, *Phys. Rev. Lett.* **131**, 161901 (2023), [arXiv:2302.04505 \[hep-lat\]](#).
- [55] N. Li, Z.-F. Sun, X. Liu, and S.-L. Zhu, Coupled-channel analysis of the possible  $D^{(*)}D^{(*)}$ ,  $\bar{B}^{(*)}\bar{B}^{(*)}$  and  $D^{(*)}\bar{B}^{(*)}$  molecular states, *Phys. Rev. D* **88**, 114008 (2013), [arXiv:1211.5007 \[hep-ph\]](#).
- [56] Q. Wang, V. Baru, A. A. Filin, C. Hanhart, A. V. Nefediev, and J. L. Wryn, Line shapes of the  $Z_b(10610)$  and  $Z_b(10650)$  in the elastic and inelastic channels revisited, *Phys. Rev. D* **98**, 074023 (2018), [arXiv:1805.07453 \[hep-ph\]](#).
- [57] A. Matsuyama, T. Sato, and T. S. H. Lee, Dynamical coupled-channel model of meson production reactions in the nucleon resonance region, *Phys. Rept.* **439**, 193 (2007), [arXiv:nucl-th/0608051](#).
- [58] J.-J. Wu, T. S. H. Lee, and B. S. Zou, Nucleon Resonances with Hidden Charm in Coupled-Channel Models, *Phys. Rev. C* **85**, 044002 (2012), [arXiv:1202.1036 \[nucl-th\]](#).
- [59] J.-J. Wu, T.-S. H. Lee, A. W. Thomas, and R. D. Young, Finite-volume Hamiltonian method for coupled channel interactions in lattice QCD, *Phys. Rev. C* **90**, 055206 (2014), [arXiv:1402.4868 \[hep-lat\]](#).
- [60] Z.-W. Liu, W. Kamleh, D. B. Leinweber, F. M. Stokes, A. W. Thomas, and J.-J. Wu, Hamiltonian effective field theory study of the  $N^*(1535)$  resonance in lattice QCD, *Phys. Rev. Lett.* **116**, 082004 (2016), [arXiv:1512.00140 \[hep-lat\]](#).
- [61] S. Aoyama, T. Myo, K. Katō, and K. Ikeda, The complex scaling method for many-body resonances and its applications to three-body resonances, *Progress of Theoretical Physics* **116**, 1 (2006).
- [62] T. Myo, Y. Kikuchi, H. Masui, and K. Katō, Recent development of complex scaling method for many-body resonances and continua in light nuclei, *Prog. Part. Nucl. Phys.* **79**, 1 (2014), [arXiv:1410.4356 \[nucl-th\]](#).
- [63] N. Moiseyev, Quantum theory of resonances: calculating energies, widths and cross-sections by complex scaling, *Physics reports* **302**, 212 (1998).
- [64] Z. Yang, G.-J. Wang, J.-J. Wu, M. Oka, and S.-L. Zhu, Novel Coupled Channel Framework Connecting the Quark Model and Lattice QCD for the Near-threshold Ds States, *Phys. Rev. Lett.* **128**, 112001 (2022), [arXiv:2107.04860 \[hep-ph\]](#).
- [65] Z. Yang, G.-J. Wang, J.-J. Wu, M. Oka, and S.-L. Zhu, The investigations of the P-wave  $B_s$  states combining quark model and lattice QCD in the coupled channel framework, *JHEP* **01**, 058, [arXiv:2207.07320 \[hep-lat\]](#).
- [66] A. Le Yaouanc, L. Oliver, O. Pene, and J. C. Raynal, Strong Decays of psi-prime-prime (4.028) as a Radial Excitation of Charmonium, *Phys. Lett. B* **71**, 397 (1977).
- [67] R. Kokoski and N. Isgur, Meson Decays by Flux Tube Breaking, *Phys. Rev. D* **35**, 907 (1987).
- [68] P. R. Page, Excited charmonium decays by flux tube breaking and the psi-prime anomaly at CDF, *Nucl. Phys. B* **446**, 189 (1995), [arXiv:hep-ph/9502204](#).
- [69] H. G. Blundell, Meson properties in the quark model: A look at some outstanding problems, (1996), [arXiv:hep-ph/9608473](#).
- [70] E. S. Ackleh, T. Barnes, and E. S. Swanson, On the mechanism of open flavor strong decays, *Phys. Rev. D* **54**, 6811 (1996), [arXiv:hep-ph/9604355](#).
- [71] D. Morel and S. Capstick, Baryon meson loop effects on the spectrum of nonstrange baryons, (2002), [arXiv:nucl-th/0204014](#).
- [72] P. G. Ortega, J. Segovia, D. R. Entem, and F. Fernandez, Molecular components in P-wave charmed-strange mesons, *Phys. Rev. D* **94**, 074037 (2016), [arXiv:1603.07000 \[hep-ph\]](#).
- [73] E. Braaten and M. Kusunoki, Decays of the X(3872) into J/psi and light hadrons, *Phys. Rev. D* **72**, 054022 (2005), [arXiv:hep-ph/0507163](#).
- [74] D. Gamermann, J. Nieves, E. Oset, and E. Ruiz Arriola, Couplings in coupled channels versus wave functions: ap-

- plication to the  $X(3872)$  resonance, *Phys. Rev. D* **81**, 014029 (2010), [arXiv:0911.4407 \[hep-ph\]](#).
- [75] L. Meng, G.-J. Wang, B. Wang, and S.-L. Zhu, Revisit the isospin violating decays of  $X(3872)$ , *Phys. Rev. D* **104**, 094003 (2021), [arXiv:2109.01333 \[hep-ph\]](#).
- [76] K. Abe *et al.* (Belle), Evidence for  $X(3872) \rightarrow \gamma J/\psi$  and the sub-threshold decay  $X(3872) \rightarrow \omega J/\psi$  (2005) [arXiv:hep-ex/0505037](#).
- [77] K. Abe *et al.* (Belle), Observation of a new charmonium state in double charmonium production in  $e^+e^-$  annihilation at  $s^{*}(1/2) \sim 10.6$ -GeV, *Phys. Rev. Lett.* **98**, 082001 (2007), [arXiv:hep-ex/0507019](#).
- [78] M. Aghasyan *et al.* (COMPASS), Search for muoproduction of  $X(3872)$  at COMPASS and indication of a new state  $\tilde{X}(3872)$ , *Phys. Lett. B* **783**, 334 (2018), [arXiv:1707.01796 \[hep-ex\]](#).
- [79] Z.-G. Wang, Analysis of the Hidden-charm Tetraquark molecule mass spectrum with the QCD sum rules, *Int. J. Mod. Phys. A* **36**, 2150107 (2021), [arXiv:2012.11869 \[hep-ph\]](#).
- [80] X.-K. Dong, F.-K. Guo, and B.-S. Zou, A survey of heavy-antiheavy hadronic molecules, *Progr. Phys.* **41**, 65 (2021), [arXiv:2101.01021 \[hep-ph\]](#).
- [81] P. G. Ortega, D. R. Entem, and F. Fernández, Does the  $J^{PC} = 1^{+-}$  counterpart of the  $X(3872)$  exist?, *Phys. Lett. B* **829**, 137083 (2022), [arXiv:2111.02475 \[hep-ph\]](#).